Volume 61
Number 9
28 January 2025
Pages 1707–1920

ChemComm

Chemical Communications

rsc.li/chemcomm

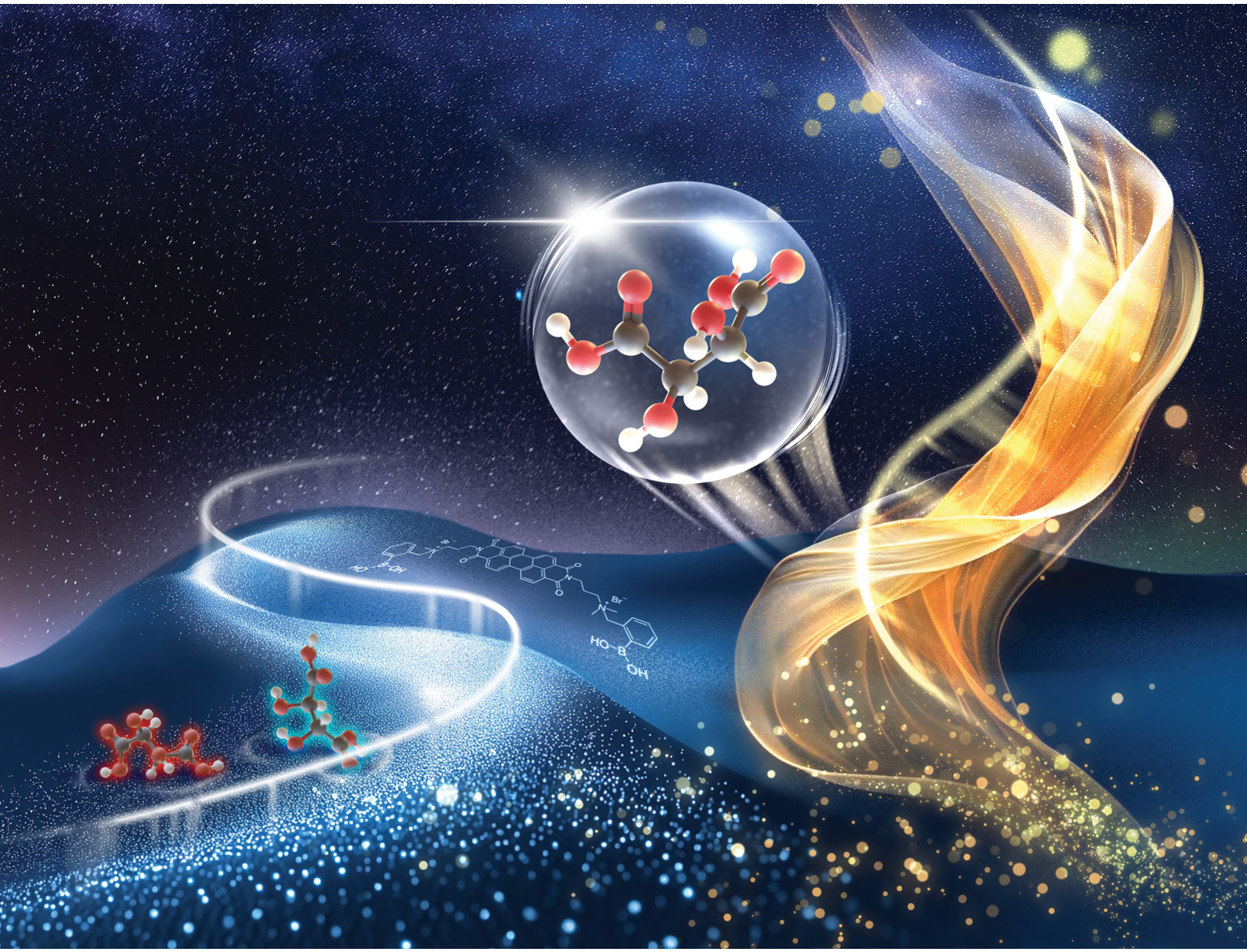

ISSN 1359-7345

ROYAL SOCIETY OF CHEMISTRY

COMMUNICATION

Yun-Bao Jiang *et al.*

Developing chiral aggregates exhibiting anti-S-shaped CD-ee dependence: using a *meso*-isomer to tune dynamic aggregates induced by enantiomers

ChemComm

ROYAL SOCIETY OF CHEMISTRY

COMMUNICATION

View Article Online
View Journal | View Issue

Cite this: *Chem. Commun.*, 2025, **61**, 1818

Received 10th October 2024,
Accepted 4th December 2024

DOI: 10.1039/d4cc05345a

rsc.li/chemcomm

Developing chiral aggregates exhibiting anti-S-shaped CD-ee dependence: using a *meso*-isomer to tune dynamic aggregates induced by enantiomers†

Xiao-Yan Lin,‡ Jin-Ling Shi,‡ Qian Wang, Yue-Bo Yu, Xuan-Xuan Chen, Xiaosheng Yan, Xin Wu, Jian-Bin Lin, Zhao Li and Yun-Bao Jiang *

We report the use of the *meso*-isomer of tartaric acid, *meso*-tartaric acid, to tune the chirality of the dynamic aggregates of a perylenebisimide dye bearing boronic acid groups in the presence of enantiomeric L-/D-tartaric acid. The CD-ee dependence changes from S- to anti-S-shaped. A change in the structures of the chiral aggregates led by the *meso*-tartaric acid is identified.

Supramolecular chirality can be described in terms of the dependence of the CD of the supramolecular system as a function of ee (enantiomeric excess) of the chiral building block or chiral inducer in the case of achiral building blocks.[1] In general, the CD-ee curve could be of three shapes, *i.e.* linear, S- and anti-S-shaped. In the majority of cases, a linear dependence is observed, which means that the two enantiomers function independently, while the S-shaped dependence, termed as to the "Majority-rules effect (MRE)",[2] means that the CD signal is higher in number than that expected for a linear dependence, suggesting a chiral amplification. However, the anti-S-shaped dependence, termed as to the "Racemate-rules effect", is much less seen.[1,3,4] In those cases in supramolecular systems the enantiomers prefer to function as a pair[3a,4] and this is somewhat similar to heterochiral preference.[5]

Based on this assumption on the origin of the anti-S-shaped CD-ee dependence, we proposed that using a *meso*-isomer, in conjunction with its enantiomer pair, to induce the aggregation of a dye, it would be possible that the generated chiral aggregates exhibit an anti-S-shaped CD-ee dependence. We succeeded in creating such chiral aggregates of perylinebisimide (PBI)-based diguanidinium in the presence of LL-, DD-, and LD-dicarboxylates *in situ* generated from the reaction of *m*-phthalaldehyde with chiral amino acids.[6] Because of the dynamic character of the imine bond in the formed dicarboxylate in exchanging with the amine precursors, the function of the *meso*-isomer, LD-dicarboxylate, could not be well understood. We thus took a *meso*-isomer of the dicarboxylate, the tartaric acid dibenzoyl ester,[7] and observed the anti-S-shaped CD-ee dependence. That, however, exists only when the *meso*-isomer co-exists with its enantiomer pair in the solution of the achiral PBI-dye; later introduction of the *meso*-isomer into the solution of the chiral aggregates induced by its enantiomers does not lead to the anti-S-shaped CD-ee curve or any changes in the absorption and CD spectra.[7] The guanidinium–carboxylate interactions, both of electrostatic and hydrogen bonding nature,[8] appear in this case not that dynamic. It would thus be of significance to explore if the chiral aggregates induced by dynamic interactions between the achiral dye building blocks and the chiral inducer would exhibit a change in the shape of the CD-ee curve, from S- to anti-S-shaped, by introducing the *meso*-isomer of the chiral inducer. Interaction of boronic acid with α-hydroxycarboxylate[3a,3b,9] was therefore employed to examine the impact of the *meso*-isomer of tartaric acid on the supramolecular chirality of the aggregates of phenylboronic acid derived PBI dye **1** (Fig. 1) induced by its enantiomeric counterparts, D-/L-tartaric acid. We observed dynamic tuning of the CD-ee dependence from S- into anti-S-shaped by the *meso*-isomer of tartaric acid.

PBI-dye **1** (Fig. 1) was chosen following our observation that its derivative with a shorter ethylene spacer between *ortho*- or

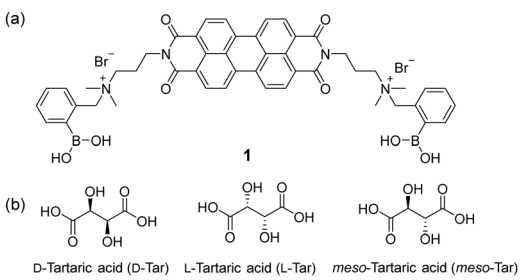

Fig. 1 Structures of PBI dye **1** (a) and tartaric acid inducers (b).

Department of Chemistry, College of Chemistry and Chemical Engineering and the MOE Key Laboratory of Spectrochemical Analysis and Instrumentation, Xiamen University, Xiamen 361005, China. E-mail: ybjiang@xmu.edu.cn

† Electronic supplementary information (ESI) available. See DOI: https://doi.org/10.1039/d4cc05345a

‡ Xiao-Yan Lin and Jin-Ling Shi contributed equally to this work.

para-phenylboronic acid and the PBI core shows a linear CD-ee dependence in its aggregates induced by D-/L-Tar.[3a] This suggests a higher helical reversal penalty (HRP) than the mismatch penalty (MMP) energies.[10] To lower the HRP, a longer and thus more flexible spacer, for example, propylene, would be employed to link the PBI core and phenylboronic acid motif. Indeed, such a PBI dye **1** showed an S-shaped dependence of CD on ee of L-/D-Tar,[3b] suggesting a chiral amplification and a lower HRP. This promoted us to explore the impact of the mesomeric counterpart of L-/D-tartaric acid on the supramolecular chirality of the aggregates of **1** induced by L-/D-tartaric acid in terms of the CD-ee dependence. The "sergeants-and-soldiers" principle (SSP) experiments[11] were first carried out to follow the CD spectra of the aggregates of **1** as a function of molar ratio of the L-Tar "sergeant" to the *meso*-Tar "soldiers" (Fig. 2). The shape of the CD spectrum remains unchanged with increasing molar ratio of *meso*-Tar up to 40%, after which a dramatic change occurs (Fig. 2a). This indicates a different structure of the aggregates induced by the *meso*-isomer compared to that induced by the enantiomer, L-tartaric acid. The *meso*-Tar induced structural change is also evident from the slight red-shift of the absorption spectrum (Fig. 2a). This is also reflected by the differed absorption and fluorescence spectra of the aggregates in the presence of L-Tar and *meso*-Tar, respectively (Fig. S1–S3, ESI†); in particular, the emission spectrum in the presence of *ca.* 1 equivalent of L-Tar exhibits a much stronger PBI excimer emission at 659 nm. At a *meso*-Tar molar ratio over 60%, the solutions turn into CD-silent, which means that *meso*-Tar disrupts the chiral aggregates of **1** originally induced by the L-Tar enantiomer. The CD signal of the aggregates of **1** in the presence of *meso*- and L-Tar of increasing molar fraction of *meso*-Tar is of a concave shape (Fig. 2b inset), which means that the CD signal is lower than that expected from the linear dependence, opposite to that of the chiral amplification.[11] A similar profile was found using the ratio of fluorescence intensity of excimer to monomer of the PBI fluorophore in **1** (Fig. S4, ESI†). This suggests that a reversal of the CD-ee dependence of the aggregates of **1** induced by enantiomers of tartaric acid would occur when the *meso*-isomer of tartaric acid is introduced.

We next monitor the CD-ee dependence of the aggregates of **1** induced by an enantiomer pair of L- and D-tartaric acid of varying ee in the presence of their *meso*-isomer, the so-called diluted MRE experiments,[11] which allows for identifying a combination of the SSP and MRE. In the absence of *meso*-Tar, the aggregates of **1** at 50 μM induced by enantiomeric L- and D-tartaric acid exhibit an S-shaped CD-ee dependence (Fig. 3a and b), a classic MRE response;[3b] the diluted MRE experiments carried out in the presence of *meso*-Tar lead to an anti-S-shaped dependence (Fig. 3d). This is accompanied by changes in the shape of the CD spectra over 360–440 nm (Fig. 3a and c), which means that the structures of the supramolecular aggregates are indeed altered upon the introduction of *meso*-Tar. This transformation from S- to anti-S-shaped CD-ee dependence takes place gradually with increasing molar fraction of *meso*-Tar from 0 to 40% (Fig. 3b, d and Fig. S5–S8, ESI†). At a higher molar fraction of *meso*-Tar, the CD signal of the aggregates becomes too weak to allow a credible CD-ee profile. We therefore succeed in building a supramolecular system that exhibits the hitherto rarely observed anti-S-shaped CD-ee dependence by introducing a *meso*-isomer into the chiral aggregates originally induced by its enantiomeric counterparts.

To understand the impact of *meso*-Tar, we compared the absorption and fluorescence spectra of the **1**/*meso*-Tar and **1**/L-Tar aggregates (Fig. S9, see also Fig. S1 and S2, ESI†). The addition of L-Tar to **1** leads to the appearance of a shoulder at 610 nm in the absorption spectrum of **1** that is assigned to the exciton coupling between coaxially stacked PBI cores (Fig. S9a, ESI†).[12] While **1** alone shows only the monomer emission characteristic of the PBI core, **1**/L-Tar shows a new emission at long wavelength of 659 nm that is assigned to the excimer of the PBI core. The **1**/*meso*-Tar also shows a long-wavelength emission at 657 nm, but it is much weaker (Fig. S9b, ESI†), implying a less effective overlapping of the π-fluorophores in

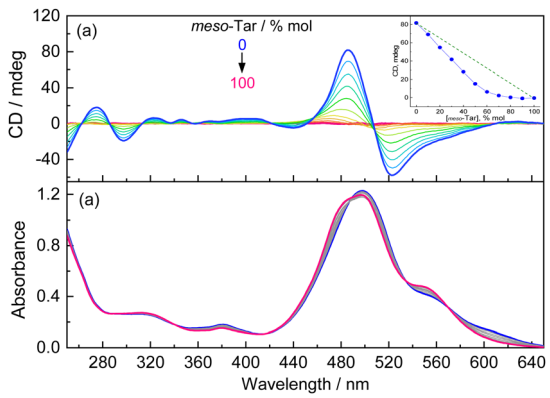

Fig. 2 Absorption and CD spectra of **1** in the presence of L-Tar and *meso*-Tar of varying molar percentage of *meso*-Tar in pH 5.0 acetate buffer containing 2.5% by volume DMSO. The inset in (a) is a plot of the CD signal at 485 nm against molar fraction of *meso*-Tar. [**1**] = 50 μM, [L-Tar] + [*meso*-Tar] = 30 μM.

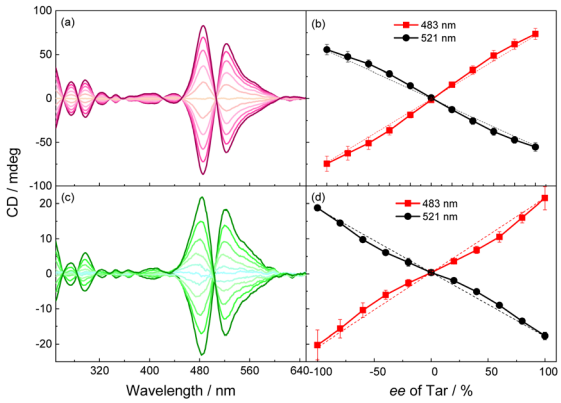

Fig. 3 CD spectra of aggregates of **1** induced by L-/D-tartaric acid of varying ee in the absence (a) and presence (c) of the *meso*-isomer of tartaric acid and plots of the CD signals at 483 nm and 521 nm *versus* ee (b) and (d). [**1**] = 50 μM, [L-Tar] + [D-Tar] = 30 μM (a) and (b); [L-Tar] + [D-Tar] = 18 μM, [*meso*-Tar] = 12 μM (c) and (d).

the assembly of **1**/*meso*-Tar. These differences in absorption and fluorescence properties indicate that the chromophores of the PBI dye stack differently in **1**/*meso*-Tar than in **1**/L-Tar (Fig. S10, ESI†). The aggregation in **1**/*meso*-Tar and **1**/L-Tar was also investigated by temperature-dependent absorption spectra (Fig. S11, ESI†). Upon cooling the sample of **1**/*meso*-Tar or **1**/L-Tar from 363 to 293 K, the maximum absorbance at 500 nm decreases while a weak transition at 600 nm appears, suggesting the formation of the classic H-aggregates of PBI.[12] The changes in the absorbance upon heating and cooling the sample solution are reversible (Fig. S11, ESI†), confirming that the changes in the structures of the aggregates are reversible.

This observation led to our exploration of the dynamic character of the aggregates of **1** in the presence of enantiomeric and *meso*-isomers of tartaric acid, for which we prepared the aggregates respectively in the "pre-mix" and "post-mix" methods (Fig. S12, ESI†). In the pre-mix method, the mixture of *meso*-Tar and L-/D-Tar is mixed with **1**, which in principle leads to co-aggregates of **1**/*meso*-/L-/D-Tar, denoted as $\mathbf{Agg1}_{pre}$. In the post-mix method, the respectively prepared **1**/*meso*-Tar aggregates and **1**/L-/D-Tar aggregates are later mixed in a given ratio, leading to aggregates denoted as $\mathbf{Agg1}_{post}$. Time-dependent CD and fluorescence studies demonstrate that $\mathbf{Agg1}_{post}$ is kinetically labile and it transforms to the same structures of $\mathbf{Agg1}_{pre}$ (Fig. S13 and S14, ESI†). This likely results from a rearrangement of the components in both aggregates, during which the CD spectral profile over 360–440 nm undergoes a change (Fig. 4a and Fig. S5–S7, ESI†), while the emission of the excimer is substantially weakened (Fig. S14, ESI†). The dependence of the CD signal of the freshly prepared **1**/Tar aggregates $\mathbf{Agg1}_{post}$ on ee of L-/D-Tar is S-shaped (Fig. 4b blue curve), in contrast to the anti-S-shaped dependence observed for $\mathbf{Agg1}_{pre}$ (Fig. 3d and Fig. 4b green curve), probably because only the aggregates of **1** containing enantiomer L- and/or D-Tar produce CD signals that account for the S-shaped CD-ee dependence. This S-shaped dependence is similar to that observed in the absence of *meso*-Tar but in the presence of L- and D-tartaric acid of the same total concentration (Fig. S15, ESI†). It is significant to note that a smooth transition from the S- to anti-S-shaped CD-ee dependence takes place when the freshly prepared $\mathbf{Agg1}_{post}$ is allowed to stand for 20 min, that the $\mathbf{Agg1}_{post}$ aggregates transform to $\mathbf{Agg1}_{pre}$ (Fig. 4a right panel and Fig. 4b red curve). This indicates that the aggregates are dynamic and undergo structural changes to arrive at the *meso*-Tar dictated aggregates eventually exhibiting the anti-S-shaped CD-ee dependence. This is different from that observed in the PBI-guanidinium/dibenzoyltartaric acid system,[7] in which the CD spectra of the post-mixed aggregates remain unchanged 40 min after mixing. We attribute the dynamic change in the structures of the aggregates of **1** in the presence of both the *meso*-isomer and enantiomer of tartaric acid to the dynamic nature of the interaction between the boronic acid moiety in dye **1** and the α-hydroxycarboxylic acid.[3a,3b,9] Our observation of this dynamic change in the structure of the aggregates suggests that the *meso*-isomer of tartaric acid is able to alter the structures of the aggregates of **1** induced by its enantiomeric counterparts, L- and D-tartaric acid.

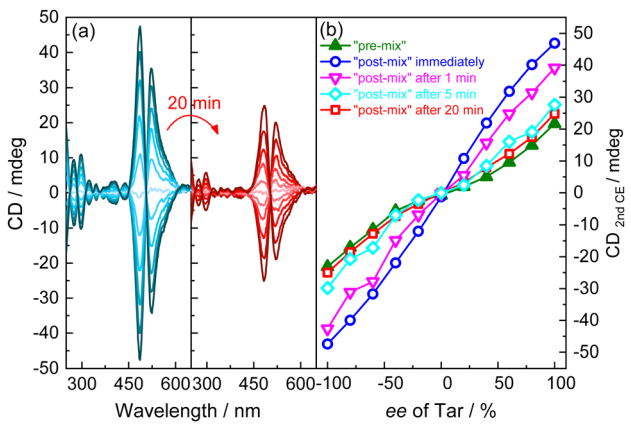

Fig. 4 (a) CD spectra of **1**/Tar aggregates prepared by the post-mix method. The resultant solutions were tested immediately upon mixed (left panel) or after standing for 1, 5, or 20 min to ensure a complete rearrangement of the building blocks (right panel). (b) CD intensity at 483 nm as a function of ee of Tar. The CD-ee curve for the "pre-mix" system is also included in (b) for comparison. [**1**] = 50 μM, [L-Tar] + [D-Tar] = 18 μM, [*meso*-Tar] = 12 μM.

We discover a new kind of aggregate that exhibits an anti-S-shaped CD-ee dependence, by introducing a *meso*-isomer to the chiral aggregates of an achiral PBI dye **1** originally induced by the enantiomeric counterparts of varying ee. This can be done either in the co-existence of *meso*-isomer and the enantiomer pair with the dye or by later mixing the respectively prepared aggregates of **1**/*meso*-isomer and aggregates of **1**/enantiomers, demonstrating that the anti-S-shaped CD-ee dependence can be achieved in dynamic aggregates, which results from the dynamic character of the interaction between the binding group incorporated in the achiral dye and the enantiomer or the *meso*-isomer. We now show that the *meso*-isomer strategy can be applied to both the static and dynamic aggregates to induce a reversal of the CD-ee dependence from S- to anti-S-shaped, which shall be of significance for our understanding of the mechanisms leading to the anti-S-shaped dependence that remains rare up until now, despite the observed effects not being very strong. More similar systems shall be found in order to well understand the mechanisms that govern the anti-S-shaped CD-ee dependence.

We greatly appreciate the support of this work by the NSF of China (grants 92356308, 22241503, 21820102006, 91856118, 21435003 and 21521004).

Data availability

All data reported in this article are provided in the main text or in the ESI† of the article.

Conflicts of interest

There are no conflicts of interest to declare.

Notes and references

1 X. Yan, Q. Wang, X.-X. Chen and Y.-B. Jiang, *Adv. Mater.*, 2020, **32**, 1905667.
2 (*a*) A. R. A. Palmans and E. W. Meijer, *Angew. Chem., Int. Ed.*, 2007, **46**, 8948–8968; (*b*) K. Toyofuku, M. A. Alam, A. Tsuda, N. Fujita, S. Sakamoto, K. Yamaguchi and T. Aida, *Angew. Chem., Int. Ed.*, 2007, **46**, 6476–6480; (*c*) T. Seki, A. Asano, S. Seki, Y. Kikkawa, H. Murayama, T. Karatsu, A. Kitamura and S. Yagai, *Chem. – Eur. J.*, 2011, **17**, 3598–3608; (*d*) C. Roche, H.-J. Sun, P. Leowanawat, F. Araoka, B. E. Partridge, M. Peterca, D. A. Wilson, M. E. Prendergast, P. A. Heiney, R. Graf, H. W. Spiess, X. Zeng, G. Ungar and V. Percec, *Nat. Chem.*, 2015, **8**, 80; (*e*) J. Kumar, H. Tsumatori, J. Yuasa, T. Kawai and T. Nakashima, *Angew. Chem., Int. Ed.*, 2015, **54**, 5943–5947.
3 (*a*) X. Wu, X.-X. Chen, B.-N. Song, Y.-J. Huang, Z. Li, Z. Chen, T. D. James and Y.-B. Jiang, *Chem. – Eur. J.*, 2014, **20**, 11793–11799; (*b*) X.-X. Chen, Y.-B. Jiang and E. V. Anslyn, *Chem. Commun.*, 2016, **52**, 12669–12671; (*c*) B. T. Herrera, S. L. Pilicer, E. V. Anslyn, L. A. Joyce and C. Wolf, *J. Am. Chem. Soc.*, 2018, **140**, 10385–10401; (*d*) We actually reported an anti-S-shaped CD-ee dependence in Ag+-cysteine coordination polymers much earlier in 2009 in a PhD thesis from this laboratory: J.-S. Shen, Supramolecular Recognition and Signalling Based on Argentophilic Metal Coordination Polymers and II-VI Group Semiconductor Photoluminescent Nanocrystals, PhD thesis, Xiamen University, 2009, p. 50, Fig. 24 (ESI†).
4 (*a*) Y. Xu, S.-L. Dong, X.-S. Yan, Q. Wang, Z. Li and Y.-B. Jiang, *Chem. Commun.*, 2021, **57**, 4311–4314; (*b*) D.-D. Tao, J.-H. Wei, X.-S. Yan, Q. Wang, B.-H. Kou, N. Chen and Y.-B. Jiang, *Chem. Commun.*, 2020, **56**, 15133–15136; (*c*) Y. Yuan, Y.-W. Xiao, X.-S. Yan, S.-X. Wu, H. Luo, J.-B. Lin, Z. Li and Y.-B. Jiang, *Chem. Commun.*, 2019, **55**, 12849–12852.
5 (*a*) M. Deng, J. Yu and D. G. Blackmond, *Nature*, 2024, **626**, 1019–1024; (*b*) X. Yan, J. Cao, H. Luo, Z. Li, Z.-X. Cao, Y. Mo and Y.-B. Jiang, *Nat. Commun.*, 2024, **15**, 9271.
6 X.-X. Chen, X.-Y. Lin, X. Wu, P. A. Gale, E. V. Anslyn and Y.-B. Jiang, *J. Org. Chem.*, 2019, **84**, 14587–14592.
7 Y. Yu, X. Lin, X. Chen, X. Yan and Y.-B. Jiang, *Sci. Sin.: Chim.*, 2020, **50**, 1844–1852.
8 (*a*) B. Iddon and C. A. Hunter, *J. Am. Chem. Soc.*, 2024, **146**, 28580; (*b*) Q. Wang, J. L. Mynar, M. Yoshida, E. Lee, M. Lee, K. Okuro, K. Kinbara and T. Aida, *Nature*, 2010, **463**, 339–343.
9 S. D. Bull, M. G. Davidson, J. M. H. van den Elsen, J. S. Fossey, A. T. A. Jenkins, Y.-B. Jiang, Y. Kubo, F. Marken, K. Sakurai, J. Zhao and T. D. Tony, *Acc. Chem. Res.*, 2013, **46**, 312–326.
10 F. Helmich, M. M. Smulders, C. C. Lee, A. P. Schenning and E. W. Meijer, *J. Am. Chem. Soc.*, 2011, **133**, 12238–12246.
11 (*a*) L. Brunsveld, B. G. G. Lohmeijer, J. A. J. M. Vekemans and E. W. Meijer, *Chem. Commun.*, 2000, 2305–2306; (*b*) T. Ishi-i, R. Kuwahara, A. Takata, Y. Jeong, K. Sakurai and S. Mataka, *Chem. – Eur. J.*, 2006, **12**, 763–776; (*c*) T. W. Anderson, J. K. M. Sanders and G. D. Pantoş, *Org. Biomol. Chem.*, 2010, **8**, 4274–4280; (*d*) S. C. Karunakaran, B. J. Cafferty, A. Weigert-Muñoz, G. B. Schuster and N. V. Hud, *Angew. Chem., Int. Ed.*, 2019, **58**, 1453–1457.
12 (*a*) J. van Gestel, *J. Phys. Chem. B*, 2006, **110**, 4365–4370; (*b*) A. J. Wilson, J. van Gestel, R. P. Sijbesma and E. W. Meijer, *Chem. Commun.*, 2006, 4404–4406; (*c*) M. M. J. Smulders, I. A. W. Filot, J. M. A. Leenders, P. van der Schoot, A. R. A. Palmans, A. P. H. J. Schenning and E. W. Meijer, *J. Am. Chem. Soc.*, 2010, **132**, 611–619.